Nano World Journal

https://doi.org/10.17756/nwj.2023-s3-116

Research Article

Open Access

Investigate the Thermal Analysis of Copper and Low Carbon Welding Through Friction Stir Welding Process

Abdullah Syed* **and Mohammad Nizamuddin Inamdar**

Faculty of Engineering and Built Environment, Lincoln University College, Malaysia

***Correspondence to:**
Abdullah Syed
Faculty of Engineering and Built Environment,
Lincoln University College,
Malaysia.
E-mail: asyed@lincoln.edu.my

Received: July 28, 2023
Accepted: October 26, 2023
Published: October 30, 2023

Citation: Syed A, Inamdar MN. 2023. Investigate the Thermal Analysis of Copper and Low Carbon Welding Through Friction Stir Welding Process. *NanoWorld J* 9(S3): S633-S636.

Published by United Scientific Group

Abstract

Through the use of the friction stir welding (FSW) procedure, the purpose of this work is to conduct research on the thermal analysis of welding copper and low carbon. Copper is a metal that is malleable, ductile, and pliable in addition to having a high level of conductivity. In addition to that, its melting point is not particularly high. In addition to this, it participates in the transfer of both heat and energy. Low-carbon steel, which is an alloy, is mostly made up of ferrous, which is a type of metal. Altering the proportion of these two components can result in a broad variety of changes to their mechanical and electrical properties. The necessary welding equipment for FSW have been designed with the help of SOLIDWORKS, and the temperature distributions across the weld zones have been analysed with the ABAQUS program. The necessary fixture for FSW is fabricated in accordance with the specifications of the machine. Tungsten carbide was employed as the material for the tools, and copper and stainless-steel type 304 were used for the foundation plates. During each trial of the FSW process, the temperature distributions throughout the weld line region of the Cu-304SS joints are recorded and analysed. With the square pin profile of a tungsten carbide tool, high ultimate tensile strength and impact strength were achieved due to the maximum temperature at weld sites. These results were achieved at a tool rotating speed of 1200 rpm, with a feed rate of 20 mm/min, and with a tungsten carbide tool.

Keywords

ABAQUS, Copper, Low carbon steel, Thermal analysis

Introduction

Every attempt at designing a structure should make an effort to avoid expenses as much as possible while maximising the use of available materials in accordance with the requirements outlined. The manufacturing of such structural systems frequently necessitates the utilisation of effective joints in order to accomplish both of the aforementioned goals. The utilization of a cutting-edge welding technique known as FSW, has been shown to be a promising candidate for the process of combining a wide variety of metallic materials.

Friction stir processing, stemming from FSW, has gained considerable attention for creating metal matrix composites on metal surfaces by incorporating reinforcement particles [1]. A novel approach involves combining friction stir processing and FSW techniques to produce FSW joints with reinforced nugget zones, where researchers have integrated nano/micro-particles into the adjacent base metals during FSW [2]. However, the incorporation of nanoparticles into dissimilar FSW has been largely unexplored. In a recent study, Tabasi et al. [3] used silicon carbide nanoparticles for dissimilar FSW between AZ31 magnesium alloy and 7075 aluminum alloy, leading to the formation of a metal matrix

composite in the weld stir zone. Similarly, [4] employed FSW to introduce silicon carbide nanoparticles into the stir zone during the dissimilar joining of AA5083 and AA6082 alloys.

Furthermore, the integration of nanoparticles into dissimilar FSW holds significant potential for advancing the performance and characteristics of welded joints, particularly in terms of mechanical properties like strength, hardness, and wear resistance [5]. This innovative approach has implications across various industries, including aerospace, automotive, and marine engineering, where lightweight yet robust materials are crucial [6]. Additionally, exploring different nanoparticle types, dispersion techniques, and their impacts on the microstructure and behavior of dissimilar friction stir welded joints presents avenues for further research and optimization in the realm of advanced materials joining [7, 8].

Because the FSW tool closes the joint gap while the welding process is taking place, there is no requirement for any additional shielding gas or smoke extraction equipment [9]. This presents a wealth of potential for the automation and integration of processes in the manufacturing sector. Welding can be accomplished with an industry standard FSW system at a traverse speed of up to 3 m/s [10]. It has been stated that the rotational speeds of tools used for steel FSW range anywhere from 100 to 1000 rpm [11]. Because of its direct influence on the friction and the heat input that occurs during FSW, the rotational speed has a direct bearing on the material's ability to soften and mix as a result of the process. When the tool is moved in the direction of the weld, the rotation of the tool results in an asymmetrical appearance of the weld profile. This is because the rotation of the tool is being superimposed on top of its translation, which results in an uneven flow of the material [12]. Position control and force control are the two methods that can be utilized to exercise control over the FSW tool. In the case of position control, the tool is positioned at a constant distance from the workpiece regardless of the forces that are being imposed on it. On the other hand, in the case of the force control technique, the traverse is due to the application of an axial force on the tool in the direction of the weld [13]. Position control differs from the force control technique in that it does not take into account the forces that are being exerted on it.

An illustration of FSW can be seen in figure 1. Because of the frictional contact between the revolving tool and the workpiece, heat is produced. This heat, in turn, softens the material around the tool, which leads to a localised plastic deformation known as metal stirring.

Methodology

Because of this, the key obstacle that needs to be overcome over the course of the welding process is the fact that it is difficult to construct the fusion welding process in such a way that zinc evaporation is achieved. Following the completion of the welding stage, a porous formation was accomplished in addition to the welded seams. As a direct consequence of this, copper and low-carbon steel both failed the test that evaluated their capacity to preserve their chemical and physical properties. Copper and low carbon steels were very carefully selected

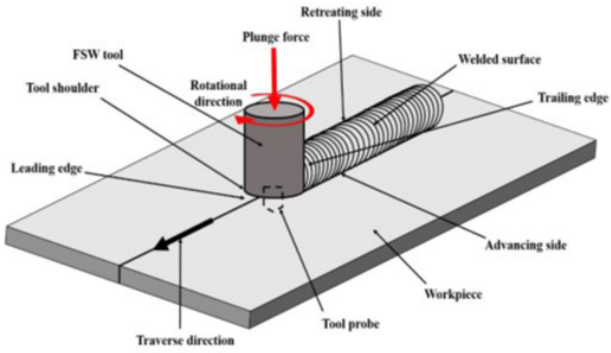

Figure 1: FSW.

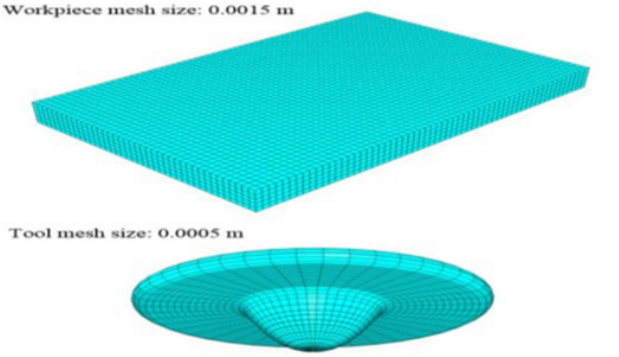

Figure 2: Surfaces of the tool and the workpiece.

as the materials to utilize in the FSW process and in the weld tool as a result of this reason.

In the beginning, a size of three millimeters was chosen for the elements in order to cut down on the amount of time spent performing numerical calculations. However, because of the disparity in the mesh of the tool and the workpiece, the size of the mesh was reduced to 1.5 millimeters in order to achieve a consistent contact between the surfaces of the tool and the workpiece, as can be seen in figure 2.

Results and Discussion

Temperature distribution

The temperature distribution of the optimised LAFSW-10 model is displayed in figure 3. This model had a traverse speed of 1500 mm/min and a rotating speed of 1800 rpm. In comparison to the models that have a traverse speed of 500 mm/min, the weld zone that is created as a result of the increased traverse speed is considerably thinner.

Heat transfer analysis

The temperature contours in the plan and cross-sectional views of the slow and fast weld models for the plunge stage are depicted in figure 3. The comparison of outcomes in the plunge stage is exclusively dependent on the rotational speed of the tool because the feed rate in the downward direction has been set as constant (100 mm/min) for both models. Because the fast weld model has a faster rotational speed than the slow weld model, the temperature in the plunge stage of

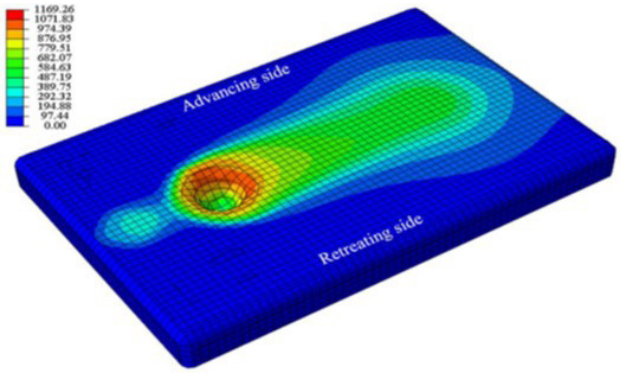

Figure 3: Temperature distribution in °C in the parametric view with increased process parameters in the LAFSW-10 model (Tool rotation: Anticlockwise direction).

the fast weld model is marginally higher than the temperature in the plunge stage of the slow weld model. The region with the greatest equivalent plastic strain was determined to be the thermomechanically impacted zone (TMAZ), and it was found to be mostly located near the interface between the tool and the workpiece, as shown in figure 4. This was demonstrated in a prior piece of study. In the case of the slow weld model, the TMAZ has a temperature that is greater than 770 °C, while the heat affected zone has a temperature that falls between 370 and 750 °C. On the other hand, in the case of the fast weld model, the TMAZ has a temperature that is greater than 889 °C, and the heat affected zone has a temperature that falls between 330 and 889 °C.

Plastic strain distribution

In this section, the plastic strain profile has been described in order to gain an understanding of the deformation that occurs throughout all stages of FSW by visualizing top and cross-sectional views of the weld. Figure 5 displays, at the plunge stage, the corresponding plastic strain distribution in the top and cross-sectional views of the slow and quick weld models. The slow weld model was used to record the maximum amount of plastic strain that could be achieved. In the model of a rapid weld shown in figure 5, an increase in rotational speed led to the development of heat, which in turn led to a reduction in the amount of friction that occurred between the tool and the workpiece due to the slip effect that occurred between them. Dubourg and colleagues have also observed the occurrence of the same phenomenon. As a direct consequence of this, a smaller amount of plastic strain was seen in the fast weld model in comparison to the slow weld model. Both the top view and the cross-sectional view demonstrate that the slow weld model possesses a significantly greater plastic strain area in comparison to the rapid weld model.

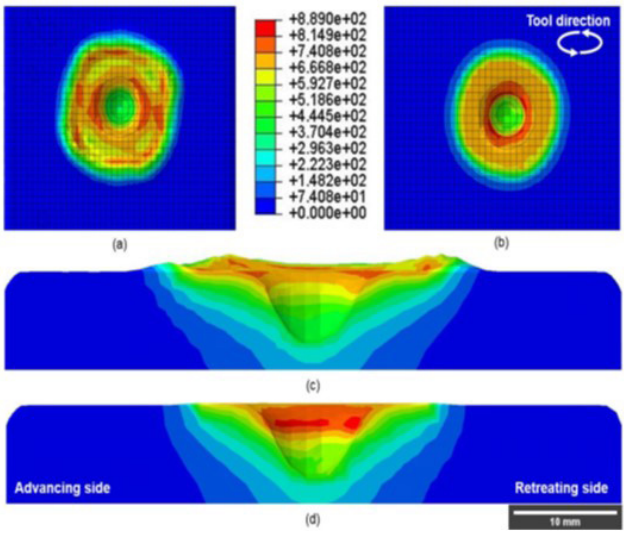

Figure 4: Temperature distribution in °C at the end of the plunge stage; **(a)** Top view of the FSW-1 model without laser heating, **(b)** Top view of the optimised LAFSW-10 model, **(c)** Cross sectional view of the FSW-1 model, and **(d)** Cross sectional view of the LAFSW-10 model. (Top views are not set according to the scale).

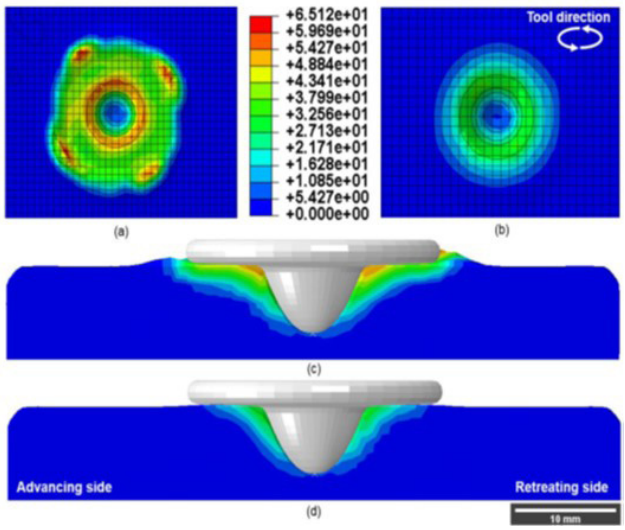

Figure 5: Temperature distribution in °C at the end of the dwell stage; **(a)** Top view of the FSW-1 model without laser heating, **(b)** Top view of the LAFSW-10 model, **(c)** Cross sectional view of the FSW-1 model, and **(d)** Cross sectional view of the LAFSW-10 model. (Top views are not set according to the scale).

Conclusions

ABAQUS has been used to construct fully coupled models of the thermomechanical and FSW variety. The findings of the research led to the discovery of the following points.

- When compared to the plunge stage of traditional FSW, reducing the tool reaction forces by pre-heating the workpiece prior to the plunge stage can lower them by up to 55%. After only five seconds of heating up, the TMAZ was able to release a substantial amount of heat for the subsequent plunge stage.
- The purpose of this study is to create a cutting tool taper that can be employed in the process of FSW of two distinct materials, namely copper and low carbon steel, at speeds of 710, 900, and 1120 rpm, respectively. Modelling is done in ABAQUS.
- Using thermal analysis, a thorough investigation into the taper tool's thermal properties, including its temperature distribution, thermal flux, gradient, and stresses, is carried out.

- Raising the speeds results in an increase in the strains that are created, and raising the speeds also results in an increase in the rates at which heat is transferred.

Acknowledgements

None.

Conflict of Interest

None.

References

1. Barmouz M, Asadi P, Givi MB, Taherishargh M. 2011. Investigation of mechanical properties of Cu/SiC composite fabricated by FSP: effect of SiC particles' size and volume fraction. *Mater Sci Eng A* 528(3): 1740-1749. https://doi.org/10.1016/j.msea.2010.11.006
2. Alidokht SA, Abdollah-Zadeh A, Soleymani S, Assadi H. 2011. Microstructure and tribological performance of an aluminium alloy based hybrid composite produced by friction stir processing. *Mater Des* 32(5): 2727-2733. https://doi.org/10.1016/j.matdes.2011.01.021
3. Tabasi M, Farahani M, Givi MB, Farzami M, Moharami A. 2016. Dissimilar friction stir welding of 7075 aluminum alloy to AZ31 magnesium alloy using SiC nanoparticles. *Int J Adv Manuf Technol* 86: 705-715. https://doi.org/10.1007/s00170-015-8211-y
4. Pantelis DI, Karakizis PN, Daniolos NM, Charitidis CA, Koumoulos EP, et al. 2016. Microstructural study and mechanical properties of dissimilar friction stir welded AA5083-H111 and AA6082-T6 reinforced with SiC nanoparticles. *Mater Manuf Process* 31(3): 264-274. https://doi.org/10.1080/10426914.2015.1019095
5. Hamdollahzadeh A, Bahrami M, Nikoo MF, Yusefi A, Givi MB, et al. 2015. Microstructure evolutions and mechanical properties of nano-SiC-fortified AA7075 friction stir weldment: the role of second pass processing. *J Manuf Process* 20: 367-373. https://doi.org/10.1016/j.jmapro.2015.06.017
6. Nikoo MF, Azizi H, Parvin N, Naghibi HY. 2016. The influence of heat treatment on microstructure and wear properties of friction stir welded AA6061-T6/Al_2O_3 nanocomposite joint at four different traveling speed. *J Manuf Process* 22: 90-98. https://doi.org/10.1016/j.jmapro.2016.01.003
7. Dragatogiannis DA, Koumoulos EP, Kartsonakis IA, Pantelis DI, Karakizis PN, et al. 2016. Dissimilar friction stir welding between 5083 and 6082 Al alloys reinforced with TiC nanoparticles. *Mater Manuf Process* 31(16): 2101-2114. https://doi.org/10.1080/10426914.2015.1103856
8. Abdollahzadeh A, Shokuhfar A, Omidvar H, Cabrera JM, Solonin A, et al. 2019. Structural evaluation and mechanical properties of AZ31/SiC nano-composite produced by friction stir welding process at various welding speeds. *Proc Inst Mech Eng Part L J Mater Des Appl* 233(5): 831-841. https://doi.org/10.1177/1464420717708485
9. Zhang YN, Cao X, Larose S, Wanjara P. 2012. Review of tools for friction stir welding and processing. *Can Metall Quart* 51(3): 250-261. https://doi.org/10.1179/1879139512Y.0000000015
10. Salih OS, Ou H, Sun W, McCartney DG. 2015. A review of friction stir welding of aluminium matrix composites. *Mater Des* 86: 61-71. https://doi.org/10.1016/j.matdes.2015.07.071
11. Dubourg L, Dacheux P. 2006. Design and properties of FSW tools: a literature review. In Proceedings of 6th International Symposium on Friction Stir Welding, Quebec, Canada.
12. Arif A, Pandey KN. 2013. Thermo-mechanical modeling for residual stresses of friction stir welding of dissimilar alloys. *Int J Eng Sci Technol* 5: 1189-1198.